Organic nanocomposite-based rotation angle sensors

KHASAN S. KARIMOV[1,2], MUHAMMAD TARIQ SAEED CHANI[3*], HADI M. MARWANI[3], ABDULLAH M. ASIRI[3]
[1]*Ghulam Ishaq Khan Institute of Engineering Sciences and Technology, Topi-23640, KPK, Pakistan*
[2]*Center for Innovative Development of Science and Technologies of Academy of Sciences, Rudaki Ave., 33, Dushanbe 734025, Tajikistan*
[3]*Center of Excellence for Advanced Materials Research, King Abdulaziz University, Jeddah 21589, P.O. Box 80203, Saudi Arabia*

The design, fabrication, and the properties of the organic nanocomposite-bsed rotation angle sensors have described in this study. The thin film of the organic semiconductor nickel phthalocyanine (NiPc), carbon nanotubes (CNTs) and silicone adhesive nanocomposite was deposited by drop casting and rubbing-in technology in the gap between two aluminum films. These aluminum films were deposited on thin plastic substrate in order to make the rotation rotation angle sensors. Experimentally, it was found that if one side of the sensor is immovable, but the second side can rotate around of longitudinal axis of the sensor at 45^o. Upon rotation in one side up to 45^o the resistance and the impedances (at 1 kHz and 200 kHz) were decreased accordingly by 1.63, 1.60 and 1.53 times due to the compression of the sensitive thin film along the length. While these parameters increased accordingly by 1.38, 1.39 and 1.46 times on the extension of the film due to rotation of the side of the sensor on 45^o in opposite side. The fabricated sensors were shockproof. The sensor's fabrication was easy; materials were cheap and ecologically friendly. The rotation angle sensors can be used as teaching aid as well.

(Received March 1, 2023; accepted October 9, 2023)

Keywords: Nanocomposite, Drop casting, Rubbing-in technique, Compression, Extension, Impedance

1. Introduction

At present a number of the rotary sensors are known e.g. the position sensor [1]. These magnetic position sensors (rotary sensors) contain housing, where the sensor is coupled with the housing, a rotor coupled with magnet is mounted (rotatably) to the housing. Moreover, the position of the magnet is adjacent to sensor. The configuring of the sensor may be done to provide the output in response to the position (rotational) of the rotor with respect to housing. A vibratory rotation sensor was presented by Loper et al. [2]. This sensor was consisted of a resonator (hemispherical), a ring-forcer electrode, number of discrete-forcer and pick-off electrodes. In the resonator a flexural or vibratory standing wave-pattern is established, and the pick-off electrodes combine the signals to produce E_c (first) and E_s (second) signals which denote the two independent constituents of the vibration pattern. In Ref. [3] the rotation rate sensors and their applications were described which can be expected in various fields such as earthquake physics and seismic tomography. The rotation sensor applications were analyzed on the base of post-seismic experimental data [4]. These experiments were linked to wave field characteristics and surface geology. The applications of rotational sensors in modal and vibration analysis of reinforced concrete beams were presented by Bońkowski et al [5]. Using novel signal-processing method the rotational speed sensors were analyzed for the accuracy improvement [6].

Currently, most of the rotational devices are based on inorganic-electronics. Organic flexible electronics are highly attractive due to their flexibility, low cost, light weight, large-area, and easy molecular tailoring to achieve required properties. Among the flexible devices the organic semiconductor-based devices have become hot and rapidly growing research field. A patent about composition and method of making a strain sensor and its use was presented by us [7]. Method of making flexible elastic conductive material and use of the same was also patented [8]. In another patent [9] the method of making and using flexible elastic nanotube composite was described. Fabrication of flexible conductive films, with semiconductive materials, formed with rubbing-in technology for elastic or deformable devices was also patented [10]. Moreover, the multifunctional pressure, displacement and temperature gradient sensor was patented as well [11].

The flexible transversal and longitudinal displacement sensor based on carbon nanotubes-CI disperse orange 25 composite were studied in Ref. [12]. The silicon composite based shock-proof and flexible multiplex sensors were fabricated by Fatima et al. [13] by using energy-free technology.

In science and engineering, the rotation angle sensors are finding applications in the fields of aircraft, automotive, medical, robotics, mining, and amusement industries. Moreover, the rotation angle sensors are also being used in consumer electronics (smart phone), seismology and structural health monitoring [14, 15].

In continuation of our efforts related the studies of the sensors [16-24] we are presenting herein the results of the fabrication and investigations of the properties of rotation angle sensors based on organic semiconductor NiPc,

carbon nanotube (CNT) and silicone adhesive composite. Moreover, the analysis of the included references showed that the data like the results presented in this paper has not been published before. The fabricated sensors may be used for the measurement of angular displacement in the shafts, gears, and steering wheels, etc.

2. Experimental

2.1. Materials

To fabricate the Al/NiPc-CNT-silicon adhesive/Al flexible rotation angle sensors the plastic sheets were used as a substrate, which had the length, width, and thickness of 3 cm, 1 cm and 0.2 mm, respectively. The sheets could be wrapped on the cylindrical body of 10 mm diameter without damaging the surface. The NiPc power was purchased from Merck-(https://www.sigmaaldrich.com/SA/en/search/nickelphthalocyanine?focus=products&page=1&pePage=30&sort=relevance&term=nickel%20phthalocyanine&type=produc) Germany, while the CNTs powder was purchased from Sun Nanotek Co. LTD (http://www.sunnano.com), China. The molecular structure of NiPc is shown in Fig. 1. The CNTs were 10 to 30 nm in diameter, while their length was in the range of 100 to 250 nm.

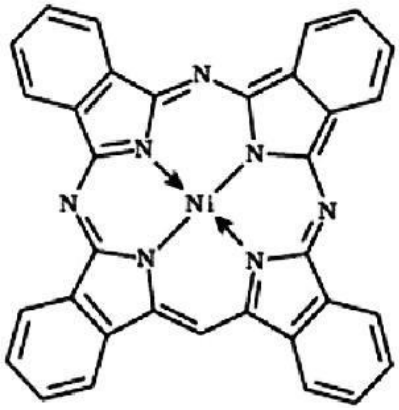

Fig. 1. Molecular structure of organic semiconductor nickel phthalocyanine

2.2. Device fabrication and characterization

The Al/NiPc-CNT-silicon adhesive/Al flexible rotation angle sensors were fabricated on the plastic sheets. The fabrication was done by the following way: thin aluminum electrodes were deposited on the plastic sheet (rubber substrate) by vacuum thermal evaporation (physical vapor deposition). The thickness of the aluminum electrodes was 50 nm. There was a gap of 0.1 mm between two aluminum electrodes. The thin organic layer of the nickel phthalocyanine (NiPc) (60 wt.%), carbon nanotube (CNT) (30 wt.%) and silicone adhesive (10 wt.%) nanocomposite was deposited in the gap between two electrodes. Prior to deposition all the components of the NiPc-CNT-silicon adhesive composite were mixed homogenously using mortar and pestle. After mixing the composite was deposited in the gap between electrodes by drop casting. Then the rubbing-in technique was used to further strengthening the bonding of NiPc-CNT-silicon adhesive nanocomposite film with the substrate. The fabricated Al/NiPc-CNT-silicon adhesive/Al flexible rotational sensors are sensitive to compression and extension forces.

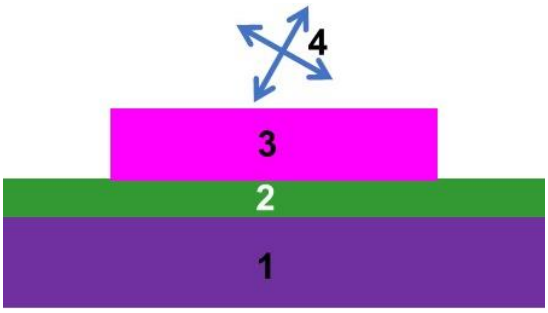

Fig. 2. Schematic diagram illustrating the rubbing-in deposition process of CNT (30 wt.%), NiPc (60 wt.%) and 10 wt.% silicon adhesive nanocomposite in the gap between Al electrodes (preliminary deposited) on the plastic substrate: plastic substrate (1), CNT, NiPc and silicon adhesive mixture film (2), polishing rubber unit (3) and (4) shows directions of the motion of the unit (3) in horizontal plane (color online)

Fig. 2 shows the schematic diagram illustrating the rubbing-in deposition process of NiPc-CNT-silicon adhesive nanocomposite film in the gap between Al films on the plastic substrate. During this process, the pressure of the CNT, NiPc and silicon adhesive depositing unit (Fig. 2) was equal to 25-35 gram/cm^2. The velocity of the movement of the unit was equal to (1-2) cm/s. Resultantly, the NiPc-CNT-silicon adhesive nanocomposite films were deposited between two aluminum electrodes on the elastic substrates. The thickness of the NiPc-CNT-silicone adhesive nanocomposite films deposited by drop-casting and rubbing-in technique on the plastic substrate were in the range of 28-34 μm.

Fig. 3 shows the schematic diagram of the rotation angle sensor based on CNT, NiPc and silicone adhesive nanocomposite. The rotation angle sensor consists of flexible substrate, aluminum electrodes, active nanocomposite film containing CNT (30 wt.%), NiPc (60 wt.%) and 10wt.% silicon adhesive, semispherical scale, rotation handle with pointer and the support. Fig. 3 shows the sensor's front view (a), top view (b) and the semispherical scale.

For the operation and testing of the rotation angle sensor the fine wires should be connected to the aluminum electrodes (2 and 3) by silver paste. Another side of the wires should be connected to measuring devices for the measurements of the resistance and impedances (at 1 kHz and 200 kHz). The resistance and the impedance were measured using MT 4090 digital LCR meter. The turning

of rotation handle (7) to clockwise or opposite direction causes rotation angle deformation of the free side on the sensor (in Fig. 3 right side) to the right or left side. Due to this the resistance (or impedance) of the CNT-NiPc-silicon adhesive nanocomposite (in Fig. 3) will increase or decrease accordingly because of the extension or compression of the sensitive layer (4 in Fig. 3) of the sensor.

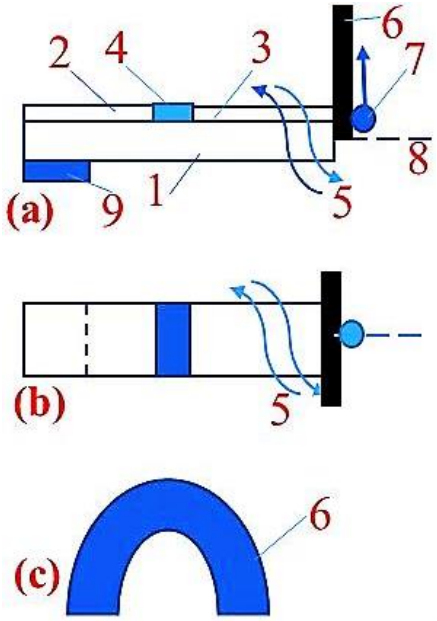

Fig. 3. Simplified schematic diagram of the rotation angle sensor based on CNT, NiPc and silicone adhesive nanocomposite: front view (a), top view (b) and semispherical scale (c): flexible substrate (1) aluminum films (2 and 3), the CNT (30 wt.%), NiPc (60 wt.%) and 10wt.% silicon adhesive (4), direction of rotation of right side of the sample (5), semispherical scale (6), rotation handle (7) with pointer, horizontal axis of sensor (8) and support (9) (color online)

3. Results and discussions

The operation of the CNT-NiPc-silicon adhesive nanocomposite-based rotation angle sensor can be made clear through the following figures. Fig. 4 shows the dependences of the resistance and impedance (at 1 kHz and 200 kHz) on rotation angle (from -45° to +45°). The increment or reduction of the resistance or impedance depends on the extension or compression of the active film. While the extension or compression depends on the rotation angle.

One side of the sensor is immovable, but the second side can rotate clockwise around of longitudinal axis of the sensor on 45°. The resistance and the impedances at 1 kHz and 200 kHz were decreased accordingly by 1.63, 1.60 and 1.53 times due to the compression of the sensitive thin film along the length. While the resistance and impedance increased accordingly by 1.38, 1.39 and 1.46 times on the extension of the film due to rotation of the side of the sensor on 45° in opposite side. The fabricated sensors are shockproof due to the presence of flexible substrate.

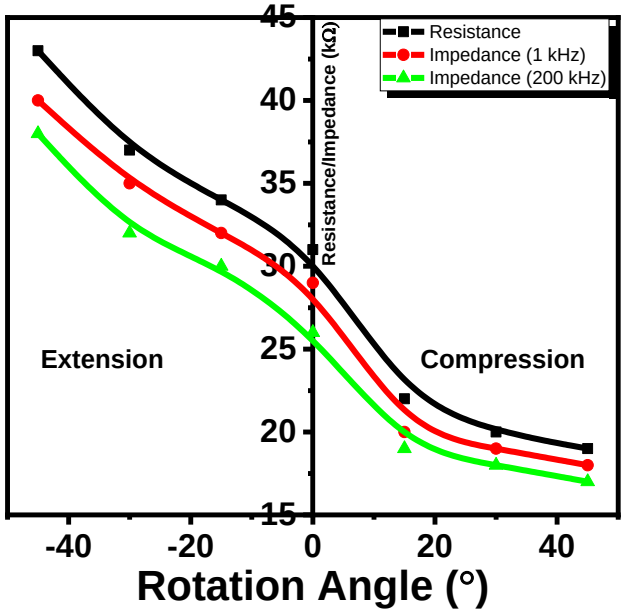

Fig. 4. Dependences of the resistance and impedance on rotation angle (color online)

Concerning the change of the resistance and impedances of the sensor we should take into consideration and differentiate the geometrical and the physical factors. The change in geometrical factors such as the lengths and cross-section of the samples causes to change the resistance and impedances. Similarly, the change in physical parameters such as conductivities takes place due to changes of the concentration and mobility of the charges accordingly at extension and compression.

For the clear understanding of the rubbing-in technology the selection of two appropriate materials based on their work functions plays a pivotal role. Likewise, the electrochemical potential (or work function) plays an important role for the materials' selection in electrochemistry. So, there are some similarities in the process which involve in electrochemistry and rubbing-in technology. Detailed information regarding this point of view may be found in the following articles [25-27].

Fig. 5 shows the dependence of the derivative of the resistance on rotation angle dR/d (angle). It is seen that the derivative at compression decreased, while at extension increased. Physically the derivative can be considered as proportional to the sensitivity of the bending sensor. It means that at extension the sensitivity of the rotation angle sensor is higher than at compression. Fig. 5 in principle has very similar behavior as Fig. 4.

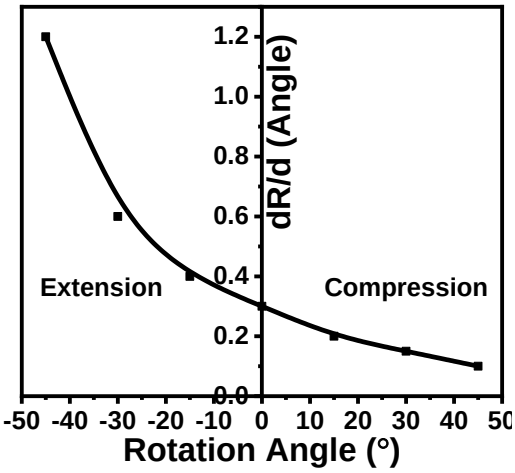

Fig. 5. Dependence of the derivative of the resistance on rotation angle dR/d(angle)

It was also found that as the frequency increased from 0 to 200 kHz the impedance decreased by 1.2 times. This behavior can be explained by using an equivalent circuit of the rotational Al/ CNT-NiPc-Si/Al sensors as parallel connection of the resistor and capacitor (Fig. 6).

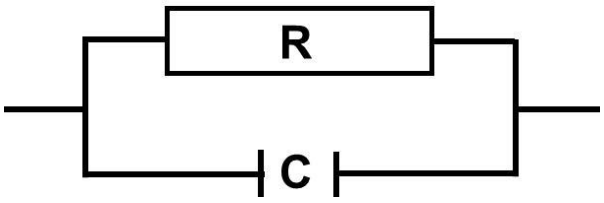

Fig. 6. Equivalent circuit of the Al/ CNT-NiPc-Si/Al rotation angle sensor

The experimental results shown in Fig. 4 may be simulated by using following mathematical function [28, 29]:

$$f(x) = e^{x} \tag{1}$$

For compression the above function (eq.1) may be represented as follows:

$$R/R_0 = e^{\theta k_1 (4\theta_m/(3\theta+\theta_m)} \tag{2}$$

where R and R_0 are the instantaneous and initial resistances. The Θ and Θ_m are the instantaneous and initial compressive angles. The k_1 is the resistance-angle coefficient, and its value was calculated as -0.0109/°.

The function given in eq. 1 can be modified for the extension as follows:

$$R/R_0 = e^{\theta k_2 ((\frac{2}{3}\theta_m + \frac{1}{3}\theta)/\theta_m)} \tag{3}$$

The value of the resistance-angle coefficient k_2 in above equation is -0.0073/°. The comparison of experimental and simulated results is given in Fig. 7. The simulated results are well matched with the experimental results. The impedance-rotation angle relationship can also be simulated using the same procedure.

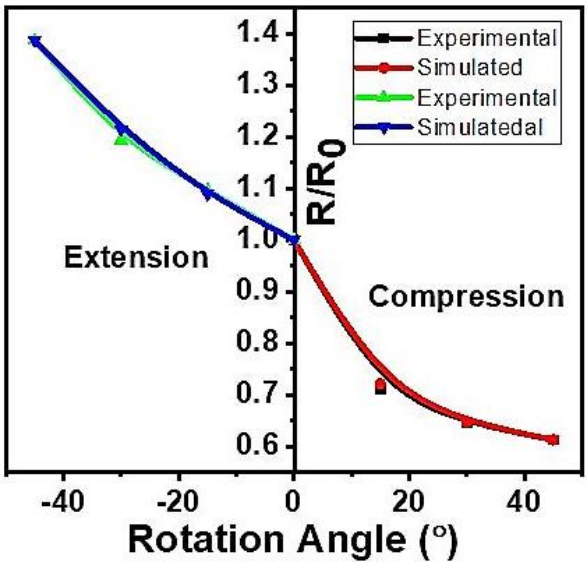

Fig. 7. The comparison of simulated and experimental results (color online)

As it is already mentioned that according to best of our knowledge the rotation angle sensors presented here are unique in design and sensing mechanism. The comparison of various rotation angle sensors based on the materials, fabrication techniques, sensing mechanism and sensitivity is given in Table 1.

Table 1. Comparison of various rotation angle sensors in terms of materials, fabrication techniques, sensing mechanism and sensitivity

Sr. No	Sensing materials	Fabrication Technology	Sensing mechanism	Sensitivity	Refs.
1	Metallic layers	Magnetron Sputtering	Magnetoresistive	1.5 mv/°	[15]
2	Terfenol-D and permanent magnet	------	Magnetostriction	3.9 mV/°	[30]
3	NiFe (thin film)	Sputtering	magneto-resistive	0.26%	[31]
4	NiPc-CNT-silicon adhesive	Rubbing-in Technology	Resistance/impedance change	266 Ω/°	current study

4. Conclusion

The rotation angle sensors were fabricated on the base of NiPc-CNTs-silicone adhesive nanocomposite using rubbing-in technology. The resistance and impedances (at 1 kHz and 200 kHz) of the sensors were dependent on the rotation of the sensitive unit in the range of -45° to +45°. The fabricated sensors potentially can be used in the instrumentation, devices for the measurements of the rotational motion. Fabrication of the sensors is easy and low-cost. The rotation angle sensors can be used for the teaching purposes as well. The fabricated devices are concerning the "flexible electronics".

Acknowledgement

This project was funded by the Deanship of Scientific Research (DSR), King Abdulaziz University, Jeddah, Saudi Arabia under grant no. (KEP-11-130-40). The authors, therefore, acknowledge with thanks DSR technical and financial support.

References

[1] M. LaPlaca, US Patents US7439732, (2008).
[2] E. J. Loper Jr, D. D. Lynch, US Patents, US4951508, (1990).
[3] Z. Zembaty, F. Bernauer, H. Igel, K. U. Schreiber, Sensors **21**(16), 5344 (2021).
[4] S. Sbaa, F. Hollender, V. Perron, A. Imtiaz, P.-Y. Bard, A. Mariscal, A. Cochard, A. Dujardin, Earth, Planets and Space **69**, 1 (2017).
[5] P. A. Bońkowski, P. Bobra, Z. Zembaty, B. Jędraszak, Sensors **20**, 4711 (2020).
[6] C. Liu, J.-G. Liu, R. Kennel, Journal of Physics: Conference Series, IOP Publishing **1065,** 072013 (2018).
[7] A. M. Asiri, S. B. Khan, M. T. S. Chani, K. S. Karimov, US Patents, US9,538,924 (2017).
[8] A. M. Asiri, S. B. Khan, K. S. Karimov, US Patents, US9,631,989 (2017).
[9] A. M. Asiri, S. B. Khan, M. T. S. Chani, K. Karimov, US Patents, US9847151 (2017).
[10] M. T. S. Chani, A. M. Asiri, H. Karimov, US Patents, US10,994,387 (2021).
[11] M. T. S. Chani, A. M. Asiri, K. Karimov, US Patents, US10,989,575 (2021).
[12] I. Ullah, K. S. Karimov, M. A. Ibrahim, N. Fatima, Coloration Technology **138**, 90 (2022).
[13] N. Fatima, K. S. Karimov, Sensors and Actuators A: Physical **331**, 112902 (2021).
[14] Z. Zembaty, F. Bernauer, H. Igel, K. U. Schreiber, Sensors **21**, 5344 (2021).
[15] C. Giebeler, D. J. Adelerhof, A. E. T. Kuiper, J. B. A. van Zon, D. Oelgeschläger, G. Schulz, Sensors and Actuators A: Physical **91**, 16 (2001).
[16] M. T. S. Chani, Microchimica Acta **184**, 2349 (2017).
[17] M. T. S. Chani, International Journal of Biological Macromolecules **194**, 377 (2022).
[18] M. T. S. Chani, K. S. Karimov, S. B. Khan, N. Fatima, A. M. Asiri, Ceramics International **45**, 10565 (2019).
[19] M. T. S. Chani, K. S. Karimov, H. M. Marwani, M. M. Rahman, A. M. Asiri, Applied Physics A **127**, 1 (2021).
[20] M. T. S. Chani, K. S. Karimov, H. Meng, K. M. Akhmedov, I. Murtaza, U. Asghar, S. Z. Abbass, R. Ali, A. M. Asiri, N. Nawaz, Russian Journal of Electrochemistry **55**, 1391 (2019).
[21] M. T. S. Chani, S. B. Khan, A. M. Asiri, K. S. Karimov, M. A. Rub, Journal of the Taiwan Institute of Chemical Engineers **52**, 93 (2015).
[22] K. S. Karimov, M. T. S. Chani, F. A. Khalid, Physica E: Low-dimensional Systems and Nanostructures **43**, 1701 (2011).
[23] K. S. Karimov, M. T. S. Chani, F. A. Khalid, A. Khan, R. Khan, Chinese Physics B **21**, 016102 (2012).
[24] S. B. Khan, M. T. S. Chani, K. S. Karimov, A. M. Asiri, B. Mehran, T. Rana, Talanta **120**, 443 (2014).
[25] K. Shimada, H. Kikura, H. Takahashi, R. Ikeda, Sensors **19,** 3901 (2019).
[26] R. Garg, N. K. Dutta, N. R. Choudhury, Nanomaterials **4**, 267 (2014).
[27] M. T. S. Chani, K. S. Karimov, E. M. Bukhsh, A. M. Asiri, Int. J. Electrochem. Sci. **15**, 5076 (2020).
[28] T. Croft, R. Davison, M. Hargreaves, Engineering Mathematics: A Modern Foundation for Electrical, Elctronic, and Control Engineers, Addison-Wesley, (1996).
[29] K. Sanginovich Karimov, M. T. Saeed Chani, F. Ahmad Khalid, A. Khan, Physica E: Low-dimensional Systems and Nanostructures **44**, 778 (2012).
[30] T. Sakon, T. Matsumoto, T. Komori, Sensors and Actuators A: Physical **321**, 112588 (2021).
[31] M. Akin, A. Pratt, J. Blackburn, A. Dietzel, Sensors **18**, 4392 (2018).

*Corresponding author: mtmohamad@kau.edu.sa